

Supporting Information

Influence of colloidal additivition with surfactant-free laser-generated metal nanoparticles on the microstructure of suction-cast Nd-Fe-B alloy

Jianing Liu, Ying Yang, Franziska Staab, Carlos Doñate-Buendia, Rene Streubel, Bilal Gökce, Fernando Maccari, Philipp Gabriel, Benjamin Zingsem, Detlef Spoddig, Karsten Durst, Michael Farle, Oliver Gutfleisch, Stephan Barcikowski, Konstantin Skokov, Anna R. Ziefuß*

Surface modification by colloidal nanoadditivition

Figures S1 and S2 show SEM images of modified feedstocks with different NP loading.

Both Figures show that the morphology and size of the used MQP-S feedstocks are comparable between batches, even after NP additivition. To demonstrate this, we show three overview SEM images of the powders with different NPs mass loadings in Figure S2.

With increasing Ag NP loading, the additives form islands on the micro powder. Lower NPs loading shows the NPs well dispersed on the MP surface, which can be seen in Figure S1. To show the reproducibility and robustness of the additivition technique, we processed another batch of NP additivited powders, shown in Figure S2, which show the same trend in terms of NP dispersion.

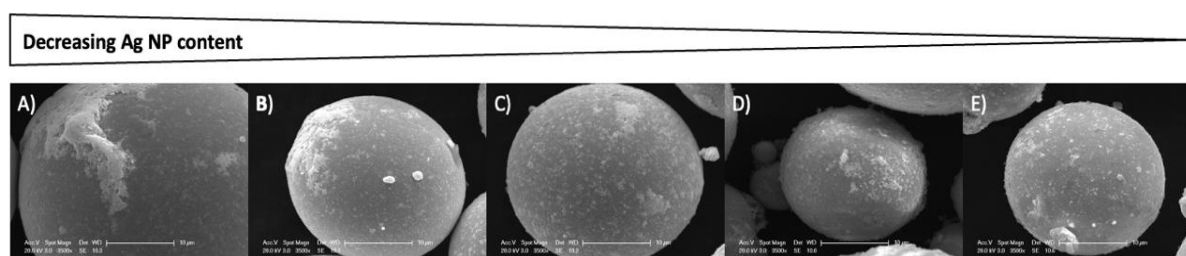


Figure S 1 SEM images of Ag NPs modified powder with different mass loads. A) 5 wt.% Ag NPs B) 2.0 wt.% Ag NPs, C) 1 wt.% Ag NPs D) 0.5 wt.% Ag NPs E) 0.1 wt.% Ag NPs.

A) 0.1 wt.% Ag NP on MQP-S B) 1.0 wt.% Ag NP on MQP-S C) 5 wt.% Ag NP on MQP-S

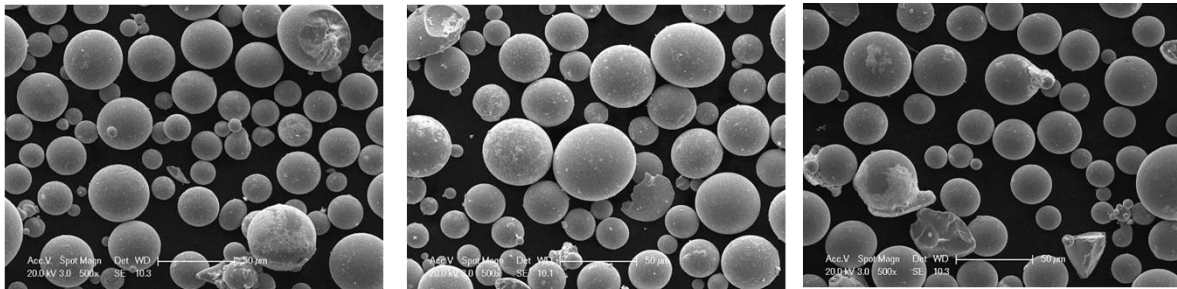


Figure S 2: SEM images of MQP-S powder modified with different mass loads of Ag NPs. A) 0.1 wt.% Ag NPs B) 1.0 wt.% Ag NPs, C) 5 wt.% Ag NPs. The images show, that the morphology of the MQP-S microparticles does not change from batch to batch and confirm the fact, that the NPs loading becomes inhomogeneous for higher mass loadings.

Hysteresis loop of the unmodified feedstock MQP-S after suction casting

The experimental procedure of the suction casting process, incl. subsequent annealing steps, can be found in the method part. The hysteresis loop of the unmodified casted part is shown in Figure S3.

Hysteresis behavior of the NP-modified feedstocks after suction casting.

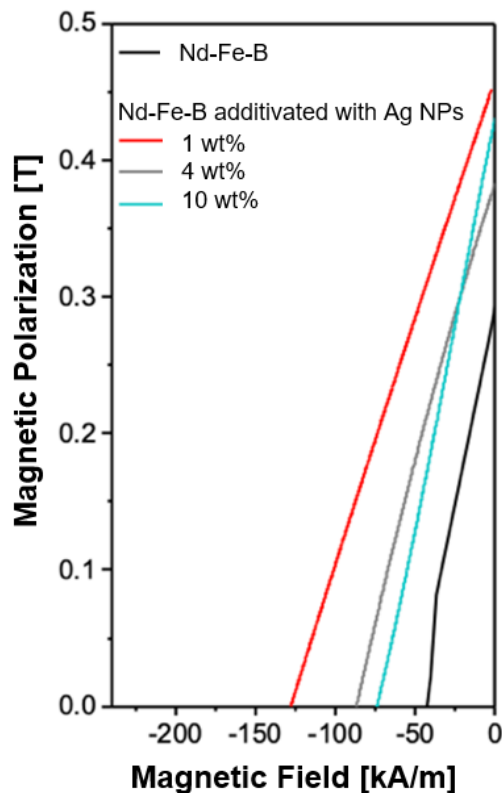


Figure S 3 Demagnetization curve of annealed suction casting samples from non-modified powder and Ag NP-modified powder at different NP mass loads.

Characterization of the composition of MQP-S

The composition of the initial feedstock powder was determined using XRF (see method section). The results are summarized in Figure S4. Note that the outcome differs slightly from the nominal composition near the stoichiometric $\text{Nd}_2\text{Fe}_{14}\text{B}$.

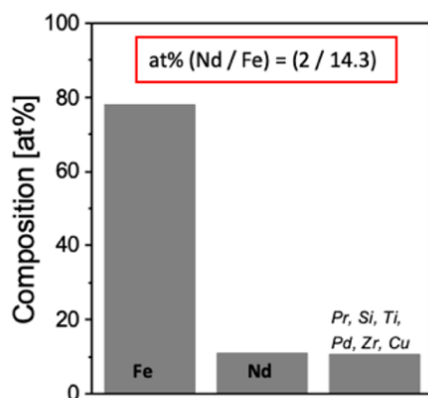


Figure S4 Chemical composition of non-additive MQP-S powder.

MQP-S microparticles size analysis

The particle size distribution of the initial feedstock powder was provided as shown in Figure S5. MQP-S is a nanocomposite powder with an average particle size around $50\ \mu\text{m}$.

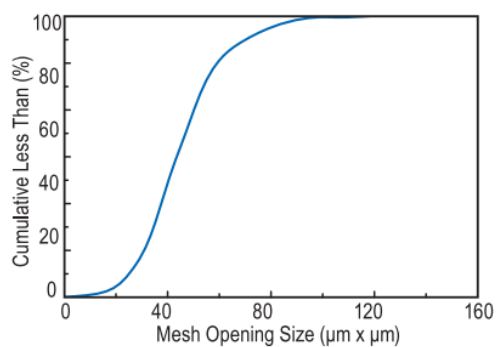


Figure S5 Particle size distribution analysis provided by the manufacturer.

Indexing rate for EBSD measurement

Table S 1 shows the indexing rate as a measure of the hit rate for each of the shown images in Figure 3 and includes the mean value and the minimum and maximum values.

Table S 1 Indexing rate for EBSD measurement.

Figure	wt. %	NP type	spot	Fraction of points in partition	Indexing rate
A	0	Ag	1	0.737	73.70%
			2	0.649	64.90%
B	0.1	Ag	1	0.699	69.90%
			2	0.732	73.20%
C	1	Ag	1	0.729	72.90%
			2	0.518	51.80%
D	7	Ag	1	0.804	80.40%
E	0.1	ZrB ₂	1	0.694	69.40%
F	1	ZrB ₂	1	0.863	86.30%
Min				0.518	51.80%
Max				0.863	86.30%
Mean				0.714	71.39%